

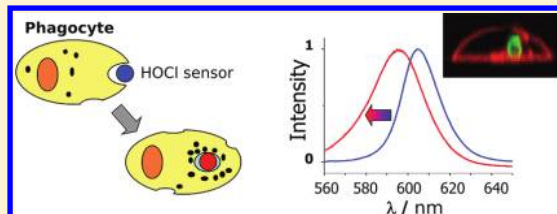
Selective and Absolute Quantification of Endogenous Hypochlorous Acid with Quantum-Dot Conjugated Microbeads

Yi-Cyun Yang, Hsueh-Han Lu, Wei-Ti Wang, and Ian Liao*

Department of Applied Chemistry and Institute of Molecular Science, National Chiao Tung University, Hsinchu, Taiwan

Supporting Information

ABSTRACT: Endogenous hypochlorous acid (HOCl) secreted by leukocytes plays a critical role in both the immune defense of mammals and the pathogenesis of various diseases intimately related to inflammation. We report the first selective and absolute quantification of endogenous HOCl produced by leukocytes *in vitro* and *in vivo* with a novel quantum dot-based sensor. An activated human neutrophil secreted $6.5 \pm 0.9 \times 10^8$ HOCl molecules into its phagosome, and kinetic measurement for the secretions showed that the extracellular generation of HOCl was temporally retarded, but the quantity eventually attained a level comparable with its intraphagosomal counterpart with a delay of about 1.5 h. The quantity of HOCl secreted from the hepatic leukocytes of rats with or without stimulation of lipopolysaccharide was also determined. These results indicate a possibility to extend our approach to not only clinical settings for quantitative assessment of the bactericidal capability of isolated leukocytes of patients but also fundamental biomedical research that requires critical evaluation of the inflammatory response of animals.



The production by living organisms of reactive oxygen species (ROS) such as superoxide radical (O_2^-), hydroxyl radical (OH^\bullet), hydrogen peroxide (H_2O_2), and hypochlorous acid (HOCl) is an inevitable fate of aerobic lives.¹ Among various endogenous ROS, the highly reactive HOCl plays a critical role in both the immune defense of mammals^{2,3} and the pathogenesis of various diseases intimately related to inflammation including atherosclerosis, atrial fibrillation, and liver cirrhosis.^{4–6} This endogenous HOCl can be produced by leukocytes of various types including abundant neutrophils that either circulate in the bloodstream or infiltrate into tissues⁷ or by tissue-specific resident macrophages such as the hepatic Kupffer cell.^{5,8} In particular, these phagocytic leukocytes can engulf invading microbes forming phagosomes and secrete HOCl into the phagosome to destroy the internalized microbe. The production of HOCl by leukocytes begins with the generation of O_2^- by reduced nicotinamide adenine dinucleotide phosphate (NADPH) oxidase; O_2^- is subsequently dismutated spontaneously or enzymatically by the superoxide dismutase to H_2O_2 . The latter is then converted to HOCl in the presence of chloride anion (Cl^-) by myeloperoxidase (MPO), a heme enzyme expressed extensively in activated leukocytes.⁹ A strict spatiotemporal regulation of HOCl is crucial; recurrent life-threatening infections can occur for patients deficient in HOCl because of defective MPO,¹⁰ but excessive production of the oxidative HOCl by either circulating or resident leukocytes might cause direct oxidative damage of the parenchymal tissue and the endothelial cell¹¹ or accelerate tissue fibrosis indirectly through activation of a key profibrotic effector, matrix metalloproteinase.⁶

Because of the pathophysiological importance of HOCl, development of a means to determine quantitatively and

selectively the secretion of endogenous HOCl is essential. As HOCl produced by leukocytes of varied types plays distinct pathophysiological roles, it is also desirable to find a means of specific determination of HOCl secreted by circulating and resident leukocytes. To this end, various sensors derived mainly from molecules have been developed;^{12–17} microorganisms that express green-fluorescence proteins have been explored to sense HOCl.^{18,19} Although some fluorescent sensors of HOCl possess satisfactory sensitivity, their selectivity is unsatisfactory as the sensor might respond to various ROS that possess sufficiently large reactivity.²⁰ A low tolerance to photobleaching of these sensors remains a hurdle for long-term imaging of cells. Furthermore, as control of the uptake of the sensors by cells is generally difficult, only a relative change, rather than an absolute quantification, of the ROS is obtainable. A lack of information about the intracellular distribution of the sensor further makes interpretation of the result obtained with these sensors elusive.

Since its invention and development, the semiconductive quantum dot (QD) has found wide biological applications because of its superior photostability and unique spectral tunability.^{21–29} Nie and co-workers reported that the emission of QD decreased significantly on exposure to HOCl.³⁰ Huang and co-workers exploited this feature and showed that the emission of QD internalized in cells diminished significantly after the cell was treated with HOCl,³¹ and we note that, instead of being produced endogenously by the cell, HOCl was added externally to the cell, and no quantitative information was

Received: August 8, 2011

Accepted: September 27, 2011

Published: September 27, 2011

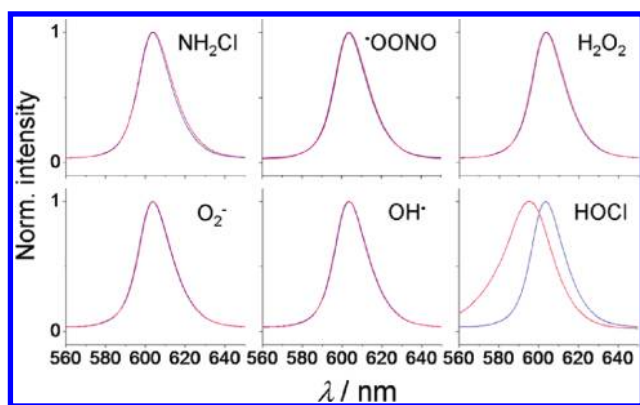


Figure 1. Emission spectra of quantum dots (QD) measured before (blue) and after (red) treatment with indicated reactive species.

explicitly reported. Here, we report the selective and absolute quantification of endogenous HOCl with a novel QD-based sensor. In contrast with conventional sensors that report ROS through varying intensity of emission, our sensing of HOCl is achieved through the unique size-spectrum relation of QD. Our sensor comprises microbeads conjugated with QD; the microbead serves as a vehicle that enables an effective control of the intracellular destination and the quantity of QD delivered to a cell. Intrapagosomal HOCl secreted by single isolated human neutrophils *in vitro* and by hepatic leukocytes of rats *in vivo* is quantified; distinct kinetics for the intrapagosomal and the extracellular secretions of HOCl have been identified. These results indicate a possibility to extend our approach to not only clinical settings for quantitative assessment of the bactericidal capability of isolated leukocytes of patients but also fundamental biomedical research that requires evaluation of the inflammatory response of animals *in vivo*.

RESULTS

Cadmium-Selenide Quantum Dots Respond Selectively to HOCl Exhibiting a Blue Shift in Their Emission. We first verified the selectivity of QD toward reactive species. We measured the emission spectrum of QD before and after subjection to treatment of six commonly found endogenous reactive species including NH_2Cl , $\cdot\text{OONO}$, H_2O_2 , $\text{O}_2\cdot^-$, $\text{OH}\cdot$, and HOCl (the preparation is described in the Supporting Information). Among the species tested, NH_2Cl , $\cdot\text{OONO}$, H_2O_2 , $\text{O}_2\cdot^-$, and $\text{OH}\cdot$ yielded no discernible variation of the spectral profile, whereas HOCl caused a significant modification of the emission spectrum, of which the wavelength at the maximum shifted from 605 to 595 nm after the treatment (Figure 1).

In seeking mechanistic insight into the spectral shift of QD induced by the treatment of HOCl, we analyzed the morphology of QD with a transmission electron (TE) microscope. The average size of the QD, determined as the length of its long axis, decreased from 8.4 ± 1.2 to 6.0 ± 1.4 nm after the treatment (Figure 2). This result conforms to the size-spectrum relation of QD and accounts satisfactorily for the blue-shifted emission of the QD observed after treatment with HOCl. The decreased size observed from the TE images indicates further that the QD were etched presumably through oxidation by HOCl, a deduction that is consistent with the conclusion drawn from measurements of mass spectra.³⁰ The selective spectral response of QD to

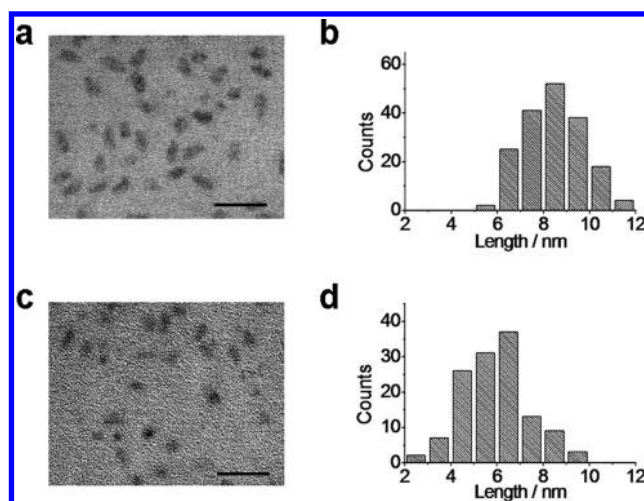


Figure 2. Morphological analysis of QD. Transmission electron micrographs and the corresponding histograms (the length of the long axis) of QD for untreated controls (a, b) and those subject to treatment with HOCl (c, d). Scale bar: 20 nm.

treatment with HOCl indicates a possibility to employ QD to determine HOCl.

HOCl Sensors Developed with Microbeads Conjugated with Quantum Dots. We designed the sensor of HOCl comprising polystyrene microbeads conjugated with QD on the surface of the microbead. We chose microbeads of diameter $2 \mu\text{m}$ to ensure that the sensor was internalized to the leukocyte through phagocytosis.³² Conjugation was achieved through formation of amide bonds between the carboxyl group on the surface of the microbead and the amino group on that of the QD (Figure 3a; the preparation is described in the Supporting Information). The highly magnified scanning electron micrographs showed that the surface of the untreated microbeads was smooth but became roughened after conjugation, and the length scale of the roughness was comparable with the size of the QD (Figure 3b). The confocal fluorescence images showed no emission from unconjugated microbeads whereas conjugated microbeads exhibited intense emission (Figure 3c). We confirmed also that the spectral profiles of the QD remained virtually the same after conjugation to the microbeads (Figure 3d). To examine the variation of the quantity of conjugated QD among microbeads, we analyzed statistically the fluorescence intensity of individual microbeads among 35 items. The coefficient of variation (C.V.) of the fluorescent intensity per microbead was less than 7.7%, indicating that the quantity of QD carried by each microbead and delivered to a leukocyte, was comparable from one to another.

We expressed the calibration curve of the sensor as the magnitude of the spectral shift, measured at varied concentrations of HOCl vs the quantity of HOCl molecules captured per microbead (Figure 3e). The latter was derived on dividing the number of HOCl molecules in the solution by the quantity of microbeads, assuming that the QD were in excess and that all HOCl had participated in the reaction (construction of the calibration curve is described in the Supporting Information). Thereafter, we derived the quantity of HOCl molecules from the magnitude of the spectral shift.

Quantification of the Intrapagosomal HOCl Secreted from Single Isolated Human Neutrophils. We first demonstrated quantification of the intrapagosomal HOCl secreted

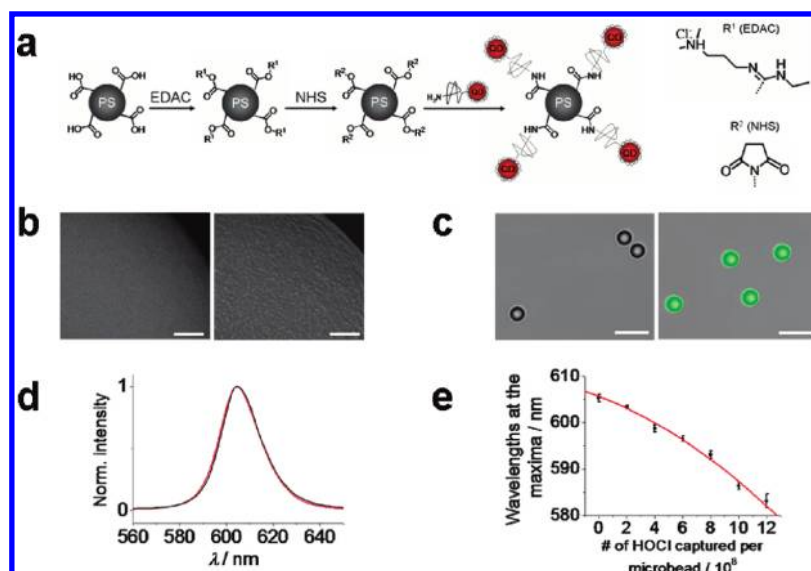


Figure 3. Preparation and characterization of QD-conjugated microbeads. (a) Cartoon illustration of a reaction scheme employed to conjugate QD to microbeads. (b) Highly magnified scanning-electron micrographs of the surface of microbeads obtained before (left) and after (right) conjugation. Scale bar: 100 nm. (c) Overlaid optical images of microbeads obtained before (left) and after (right) conjugation (green: fluorescence; gray: bright-field). Scale bar: 5 μm . (d) Emission spectra of free QD (black) and QD-conjugated microbeads (red). (e) Calibration curve (solid circles: data; red line: fitting).

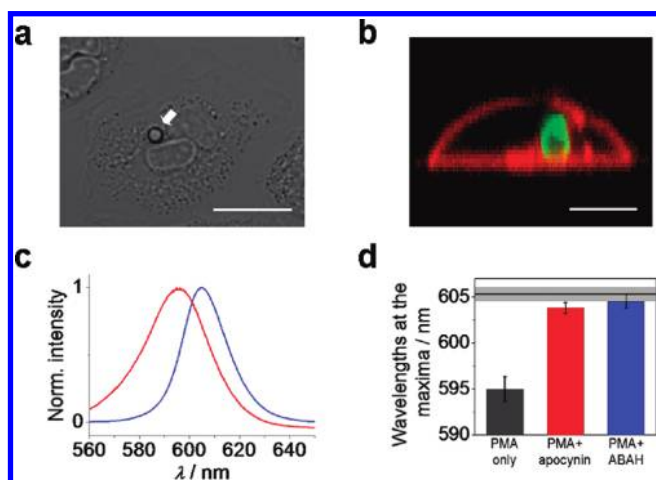


Figure 4. Determination of intraphagosomal HOCl. (a) Bright-field image showing an isolated human neutrophil and an internalized QD-decorated microbead (white arrow). Scale bar: 10 μm . (b) Cross-sectional view of dual-color fluorescence image. The green and red colors represent emission between 510 and 630 nm and between 647 and 710 nm, respectively. Scale bar: 5 μm . (c) Emission spectrum measured from a microbead in a cell-free medium (blue) and that inside a neutrophil (red). (d) Wavelengths of maximum emission measured from microbeads in neutrophils subject to indicated pretreatments (PMA only, $n = 9$; PMA and apocynin, $n = 4$; PMA and ABAH, $n = 30$).

from single human neutrophils under conditions that resemble leukocytes of healthy patients and that of patients with genetically defective ROS-production enzymes. We activated the isolated neutrophil with phorbol 12-myristate 13-acetate (PMA)³³ and then treated the activated neutrophil with microbeads that had been opsonized with human serum. The bright-field image obtained with a confocal microscope showed that a QD-decorated microbead was internalized by an activated neutrophil (Figure 4a). To verify that the microbead was indeed in the

intracellular space, we fixed the cell, labeled the cell to highlight the plasma membrane of the cell, and recorded a dual-color fluorescence image. The cross-sectional view of the cell showed unambiguously that the QD-decorated microbead was indeed engulfed by the neutrophil (Figure 4b).

We then characterized the emission spectrum of various individual internalized microbeads with a microspectrometer that had been integrated into the microscope. The emission spectrum measured from a phagocytosed microbead exhibited a blue shift relative to the control measured in a cell-free medium (595.3 nm vs 605.3 nm at wavelengths of maxima; Figure 4c). We characterized nine microbeads that had been phagocytosed with activated neutrophils. On the basis of our calibration curve, we determined that a stimulated human neutrophil secreted $6.5 \pm 0.9 \times 10^8$ HOCl molecules into its phagosome. In comparison, this value is about 6-fold higher than the quantity (LD_{90}) required to kill *S. aureus* and *E. coli*.^{9,18,34} Although leukocytes employ also antimicrobial enzymes such as elastase in addition to oxidant to combat intruding pathogens, our result indicates that the intraphagosomal generation of HOCl alone might be sufficiently effective to kill the internalized microbes.

To resemble neutrophils with a genetic defect, we challenged the cell with inhibitors of two enzymes, NADPH oxidase and MPO, which are responsible in the generation of phagocytic HOCl as stated in the introduction. In addition to mimicking defective neutrophils, the inhibitory assays served also as negative controls to verify that the spectral shift observed from the phagocytosed microbead was caused by the endogenous HOCl secreted from the neutrophil. We preloaded the neutrophil with 4'-hydroxy-3'-methoxyacetophenone (apocynin) to inhibit NADPH oxidase;³⁵ inhibition of MPO was achieved with 4-aminobenzoic acid hydrazide (ABAH).³⁶ Both experiments resulted in only a minor spectral shift (wavelengths at the maxima shifted from 605.3 ± 0.8 to 603.8 ± 0.6 nm and to 604.5 ± 0.7 nm for the apocynin and the ABAH assays, respectively) in comparison with that obtained from neutrophils without treatment with inhibitors (Figure 4d). The significantly decreased

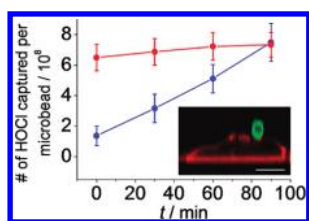


Figure 5. Kinetics of intraphagosomal (red, $n = 9$) and extracellular production (blue, $n = 8$) of HOCl from single human neutrophils. Inset: a cross-sectional image showing an unengulfed microbead that remained adhered to the membrane of a neutrophil. The color scheme is described in the legend of Figure 4b. Scale bar: $5 \mu\text{m}$.

spectral shift observed in these experiments conforms to the inhibitory effect of apocynin and ABAH and indicates the possibility of employing our HOCl sensor to examine neutrophils isolated from patients with impaired generation of HOCl. This result provides also compelling evidence to support that the spectral shift of the phagocytosed microbeads was caused by the intraphagosomal HOCl generated enzymatically by the neutrophils.

Secretion Kinetics of the Extracellular HOCl Is Distinct from Those of Its Intraphagosomal Counterpart. We attempted also to characterize the secretion kinetics by monitoring the spectral variation of single internalized microbeads. The first datum of the kinetic curve was obtained 20 min after loading the microbeads onto the cells; this duration was required to identify a completely internalized microbead and to complete a measurement. Despite the constraint, our result showed unambiguously that the initial generation of the intraphagosomal HOCl was rapid, occurring within 20 min after loading the microbead (Figure 5). Although probing the initial generation of HOCl with improved temporal precision is not yet achievable, the result is qualitatively consistent with the kinetics of the reported oxidative burst of neutrophils.¹⁰

To probe the extracellular HOCl, we employed microbeads without opsonization; these microbeads did not enter the cytoplasm of the cell and adhered only to the membrane (cf. inset of Figure 5). Our measurements show that extracellular generation of HOCl was temporally retarded, but the quantity of the extracellular HOCl eventually attained a level comparable with that of its intraphagosomal counterpart with a delay about 1.5 h (Figure 5).

Quantification of HOCl Produced from the Hepatic Leukocytes of Rats Elicited with Lipopolysaccharide. Lipopolysaccharide (LPS) is an endotoxin from Gram-negative bacteria and can induce strong immune responses in animals.³⁷ We demonstrated an in vivo application of our HOCl sensor by determining the HOCl produced from hepatic leukocytes of a rat that was elicited with LPS. We injected microbeads 2.5 h after LPS stimulation. Some injected microbeads were captured and engulfed by the hepatic leukocyte (Figure 6a). We then characterized the spectral shift and deduced the quantity of HOCl as described above. The results showed that the hepatic leukocyte of the LPS-elicited rats produced $5.9 \pm 0.8 \times 10^8$ HOCl molecules (Figure 6b), indicating that a strong immune response and enhanced inflammation in the rat liver had been induced by the injection of LPS. In comparison, the control, which was conducted in the same manner except that the LPS solution was replaced with normal saline, resulted in only moderate generation of HOCl molecules ($2.4 \pm 0.7 \times 10^8$, Figure 6b); the lesser

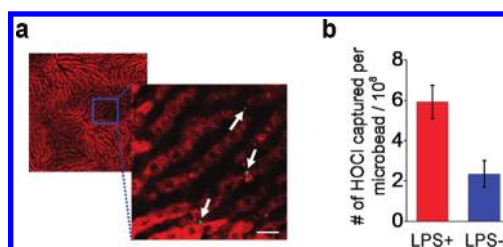


Figure 6. Determination of in vivo generation of HOCl. (a) Overlaid image showing microbeads (arrow) captured by a hepatic leukocyte of rats (red: autofluorescence of rat liver; green: fluorescence of QD). Scale bar: $20 \mu\text{m}$. (b) Quantification of HOCl secreted from hepatic leukocytes of rats with (red, $n = 14$, from three rats) or without (blue, $n = 46$, from three rats) stimulation of lipopolysaccharide (LPS).

but still significant generation of HOCl is rationalized with the immune response induced by the injected microbead itself.

DISCUSSION

This work demonstrates the first selective and absolute quantification of HOCl secreted in the phagosome at the level of single living leukocytes. As HOCl is considered to be a highly effective bactericidal reagent employed by the immune cell to defend against invading microbial pathogens, the ability to quantify HOCl produced from leukocytes indicates an unprecedented means of assessment that transcends inspection of only the phagocytic ability of leukocytes in a direct evaluation of their bactericidal functionality. This discovery opens an important application to examine patients with genetically defective MPO in their phagocytes, of whom the phagocytic activity of their phagocytes might remain normal while the ability to produce bactericidal species can be largely impaired. Our approach is expected to be extensible to clinical settings as the measurements can be readily conducted with optical microscopes or flow cytometers that are equipped with a capability of spectral measurements.

Our HOCl sensor has been tailored to determine unambiguously the quantity of the intraphagosomal HOCl secreted from single leukocytes. We deliberately chose microbeads of diameter $2 \mu\text{m}$ as a vehicle to deliver the sensing species (i.e., our QD) to ensure that QD are internalized through phagocytosis rather than other nonspecific processes such as endo- or pinocytosis. This design enables the control of not only the intracellular destination but also the quantity of the sensing species delivered to the destination, two factors that are crucial for specific and absolute quantification of the intraphagosomal HOCl. In contrast, most HOCl sensors comprise mainly small molecules and might distribute in both subcellular organelles and the cytosol, making interpretation of the result determined elusive.

In addition to the intraphagosomal HOCl secreted by phagocytic leukocytes, extracellular HOCl has been suggested to be an alternative bactericidal weapon employed by neutrophils to defend against intruding microbes.¹⁰ Despite its importance in immune defense, excessive production of extracellular HOCl is implicated in critical diseases intimately related to inflammatory disorder such as sepsis, arterial fibrillation, and atherosclerosis.^{6,38,39} Our HOCl sensor also enables determination of extracellular HOCl. In particular, we identified distinct secretion kinetics between the intraphagosomal and extracellular HOCl. As extracellular HOCl might arise from intracellular HOCl that diffused across the membrane or be produced directly by the extracellular

MPO that was secreted from the leukocyte, it is plausible that the rate of generation of extracellular HOCl is less than for its intraphagosomal counterpart. This is the first report to describe the kinetics of the generation of extracellular HOCl by leukocyte. This finding might provide clues to reveal undiscovered roles of the extracellular HOCl, improving our understanding of the innate immune defense and the complications due to mismanaged extracellular HOCl.

Injection of LPS, an endotoxin from Gram-negative bacteria, into animals such as rats is a common animal model employed in studies of inflammatory disorder caused by mismanaged generation of ROS after bacterial infection.^{40,41} In addition to the determination of HOCl produced by leukocytes isolated from whole blood, we have demonstrated quantification of HOCl secreted in vivo from the hepatic leukocyte of rats elicited with LPS. This demonstration indicates a possibility to measure endogenously produced HOCl in living animals, so opening a route to study diseases related to oxidative damage caused by HOCl.

CONCLUSION

In sum, we have developed a novel means to quantify selectively endogenous HOCl and demonstrated applications of this sensor both in vitro and in vivo. We envisage that our approach is useful for fundamental studies aiming to unravel the detailed roles played by intraphagosomal and extracellular HOCl, especially in the pathogenesis of critical diseases that intimately relate to the unregulated production of phagocytic HOCl and inflammatory disorder, such as sepsis and atherosclerosis. On the practical side, our approach can serve as a means to assess the bactericidal capability of leukocytes or to examine the strength of the immune response.

ASSOCIATED CONTENT

S Supporting Information. Experimental details and supporting data as noted in text. This material is available free of charge via the Internet at <http://pubs.acs.org>.

AUTHOR INFORMATION

Corresponding Author

*E-mail: ianliu@mail.nctu.edu.tw.

ACKNOWLEDGMENT

We thank Professors Yuan-Pern Lee and Yaw-Kuen Li (National Chiao Tung University) for generous support. We are grateful also to Professor Hsin-Yun Hsu (National Chiao Tung University) and Dr. Wei-Tien Chang (National Taiwan University Hospital) for helpful discussion. National Science Council and the MOE-ATU program of Taiwan provided support to I.L.

REFERENCES

- (1) Finkel, T.; Holbrook, N. J. *Nature* **2000**, *408*, 239–247.
- (2) Roos, D.; Winterbourn, C. C. *Science* **2002**, *296*, 669–671.
- (3) Fang, F. C. *Nat. Rev. Microbiol.* **2004**, *2*, 820–832.
- (4) Daugherty, A.; Dunn, J. L.; Rateri, D. L.; Heinecke, J. W. *J. Clin. Invest.* **1994**, *94*, 437–444.
- (5) Nahon, P.; Sutton, A.; Rufat, P.; Zioli, M.; Akouche, H.; Laguillier, C.; Charneau, N.; Ganne-Carrie, N.; Grandjean-Lemaire, V.;

N'Kontchou, G.; Trinchet, J.-C.; Gattegno, L.; Pessayre, D.; Beaugrand, M. *Hepatology* **2009**, *50*, 1484–1493.

(6) Rudolph, V.; Andrie, R. P.; Rudolph, T. K.; Friedrichs, K.; Klinke, A.; Hirsch-Hoffmann, B.; Schwoerer, A. P.; Lau, D.; Fu, X. M.; Klingel, K.; Sydow, K.; Didie, M.; Seniuk, A.; von Leitner, E. C.; Szoecs, K.; Schrickel, J. W.; Treede, H.; Wenzel, U.; Lewalter, T.; Nickenig, G.; Zimmermann, W. H.; Meinertz, T.; Boger, R. H.; Reichenspurner, H.; Freeman, B. A.; Eschenhagen, T.; Ehmke, H.; Hazen, S. L.; Willems, S.; Baldus, S. *Nat. Med.* **2010**, *16*, 470–475.

(7) Hasegawa, T.; Malle, E.; Farhood, A.; Jaeschke, H. *Am. J. Physiol.-Gastrointest. Liver Physiol.* **2005**, *289*, G760–G767.

(8) Rensen, S. S.; Slaats, Y.; Nijhuis, J.; Jans, A.; Bieghs, V.; Driessen, A.; Malle, E.; Greve, J. W.; Buurman, W. A. *Am. J. Pathol.* **2009**, *175*, 1473–1482.

(9) Nauseef, W. M. *Immunol. Rev.* **2007**, *219*, 88–102.

(10) Klebanoff, S. J. *J. Leukocyte Biol.* **2005**, *77*, 598–625.

(11) Weiss, S. J. *N. Engl. J. Med.* **1989**, *320*, 365–376.

(12) Kenmoku, S.; Urano, Y.; Kojima, H.; Nagano, T. *J. Am. Chem. Soc.* **2007**, *129*, 7313–7318.

(13) Shepherd, J.; Hilderbrand, S. A.; Waterman, P.; Heinecke, J. W.; Weissleder, R.; Libby, P. *Chem. Biol.* **2007**, *14*, 1221–1231.

(14) Sun, Z. N.; Liu, F. Q.; Chen, Y.; Tam, P. K. H.; Yang, D. *Org. Lett.* **2008**, *10*, 2171–2174.

(15) Freitas, M.; Lima, J.; Fernandes, E. *Anal. Chim. Acta* **2009**, *649*, 8–23.

(16) Yang, Y. K.; Cho, H. J.; Lee, J.; Shin, I.; Tae, J. *Org. Lett.* **2009**, *11*, 859–861.

(17) Chen, S. M.; Lu, J. X.; Sun, C. D.; Ma, H. M. *Analyst* **2010**, *135*, 577–582.

(18) Palazzolo, A. M.; Suquet, C.; Konkel, M. E.; Hurst, J. K. *Biochemistry* **2005**, *44*, 6910–6919.

(19) Schwartz, J.; Leidal, K. G.; Femling, J. K.; Weiss, J. P.; Nauseef, W. M. *J. Immunol.* **2009**, *183*, 2632–2641.

(20) Halliwell, B.; Whiteman, M. *Br. J. Pharmacol.* **2004**, *142*, 231–255.

(21) Brus, L. E. *J. Chem. Phys.* **1984**, *80*, 4403–4409.

(22) Hines, M. A.; Guyot-Sionnest, P. *J. Phys. Chem.* **1996**, *100*, 468–471.

(23) Chan, W. C. W.; Nie, S. M. *Science* **1998**, *281*, 2016–2018.

(24) Bruchez, M.; Moronne, M.; Gin, P.; Weiss, S.; Alivisatos, A. P. *Science* **1998**, *281*, 2013–2016.

(25) Jaiswal, J. K.; Mattoussi, H.; Mauro, J. M.; Simon, S. M. *Nat. Biotechnol.* **2003**, *21*, 47–51.

(26) Larson, D. R.; Zipfel, W. R.; Williams, R. M.; Clark, S. W.; Bruchez, M. P.; Wise, F. W.; Webb, W. W. *Science* **2003**, *300*, 1434–1436.

(27) Somers, R. C.; Bawendi, M. G.; Nocera, D. G. *Chem. Soc. Rev.* **2007**, *36*, 579–591.

(28) Gill, R.; Zayats, M.; Willner, I. *Angew. Chem., Int. Ed.* **2008**, *47*, 7602–7625.

(29) Biju, V.; Itoh, T.; Ishikawa, M. *Chem. Soc. Rev.* **2010**, *39*, 3031–3056.

(30) Mancini, M. C.; Kairdolf, B. A.; Smith, A. M.; Nie, S. M. *J. Am. Chem. Soc.* **2008**, *130*, 10836–10837.

(31) Yan, Y.; Wang, S. H.; Liu, Z. W.; Wang, H. Y.; Huang, D. J. *Anal. Chem.* **2010**, *82*, 9775–9781.

(32) Champion, J. A.; Walker, A.; Mitragotri, S. *Pharm. Res.* **2008**, *25*, 1815–1821.

(33) Wolfson, M.; McPhail, L. C.; Nasrallah, V. N.; Snyderman, R. *J. Immunol.* **1985**, *135*, 2057–2062.

(34) Chapman, A. L. P.; Hampton, M. B.; Senthilmohan, R.; Winterbourn, C. C.; Kettle, A. J. *J. Biol. Chem.* **2002**, *277*, 9757–9762.

(35) Stolk, J.; Hiltermann, T. J. N.; Dijkman, J. H.; Verhoeven, A. J. *Am. J. Respir. Cell Mol. Biol.* **1994**, *11*, 95–102.

(36) Kettle, A. J.; Gedye, C. A.; Winterbourn, C. C. *Biochem. J.* **1997**, *321*, 503–508.

(37) Xing, Z.; Jordana, M.; Kirpalani, H.; Driscoll, K. E.; Schall, T. J.; Gauldie, J. *Am. J. Respir. Cell Mol. Biol.* **1994**, *10*, 148–153.

- (38) Malle, E.; Waeg, G.; Schreiber, R.; Grone, E. F.; Sattler, W. S.; Grone, H. J. *Eur. J. Biochem.* **2000**, *267*, 4495–4503.
- (39) Babior, B. M. *Am. J. Med.* **2000**, *109*, 33–44.
- (40) Wang, X. Z.; Suzuki, Y.; Tanigaki, T.; Rank, D. R.; Raffin, T. A. *Am. J. Respir. Crit. Care Med.* **1994**, *150*, 1449–1452.
- (41) Suntres, Z. E.; Shek, P. N. *Shock* **1996**, *6*, S57–S64.